Available online at www.sciencedirect.com
ScienceDirect
Polymer 48 (2007) 2892–2900
polymer
www.elsevier.com/locate/polymer

Synergic flame retardancy mechanism of montmorillonite in the nano-sized hydroxyl aluminum oxalate/LDPE/EPDM system

Zhi-Hong Chang [a], Fen Guo [a,*], Jian-Feng Chen [a], Lei Zuo [b], Jiang-Hua Yu [c], Guo-Quan Wang [c]

[a] *Key Laboratory for Nanomaterials, Ministry of Education; Research Center of the Ministry of Education for High Gravity Engineering and Technology, Department of Chemical Engineering, Beijing University of Chemical Technology, 15 BeiSanhuan East Road, Chao Yang District, Beijing 100029, China*
[b] *School of Science, Beijing University of Chemical Technology, Beijing 100029, China*
[c] *Institute of Material Science and Engineering, Beijing University of Chemical Technology, Beijing 100029, China*

Received 30 October 2006; received in revised form 15 March 2007; accepted 17 March 2007
Available online 21 March 2007

Abstract

Nano-sized hydroxyl aluminum oxalate (nano-HAO) and montmorillonite (MMT) were mixed into low density polyethylene (LDPE)/ethylene propylene diene rubber (EPDM) system via melt compounding method. By means of LOI and UL94 horizontal burning tests, MMT and nano-HAO together exhibited better performance on flame-retarding LDPE/EPDM composites than how they performed individually, which proved that there existed a synergistic effect between MMT and nano-HAO on flame retardancy. Furthermore, through the analysis of Fourier transform IR spectra (FTIR), scanning electron microscope (SEM), and the thermogravimetric and differential thermal analysis (TG–DTA), the mechanism of the synergistic flame retardance was proposed as when MMT was added into nano-HAO/LDPE/EPDM composites, a laminated structure formed in the char layer and thus the transmission speeds of heat, oxygen, flammable mass and vapor were adjusted. So the process of combustion was retarded owing to lack of oxygen and heat.

Keywords: Hydroxyl aluminum oxalate (HAO); Montmorillonite (MMT); Flame retardancy

1. Introduction

Polymeric materials have made an important role in electrical engineering for long time, owing to their excellent insulation properties and mechanical properties. The application of polymeric materials in this field, however, requires special precautions because fire can be generated easily. Thus the studies on flame-retarding polymeric materials become indispensable when these materials are widely used. There are four factors affecting the process of combustion, which are oxygen, heat, flammable materials and reaction of thermal degradation [1]. Flame retardants were accordingly used against these four factors to extinguish the fire.

Brominated flame retardants, which stop the thermal degradation of composites by reacting with the polymers, are the most effective flame retardants [2–4] in markets and are adopted by most engineering plastics [5–7]. However, halogen flame retardants can release toxic gas when they suffer high temperature. With the proposal of the concept of environmentally friendly flame retardants, some brominated flame retardants begin to be replaced by some halogen-free flame retardants, particularly metallic hydroxide flame retardants (such as magnesium hydroxide [8], aluminum trihydrate [9], hydrotalcite [10], magnesium hydroxide sulfate hydrate whisker [11]).

In these metallic hydroxide flame retardants, aluminum trihydrate (ATH) is one of the most popular, safe, halogen-free flame retardant and smoke suppressant with numerous benefits, such as low material costs, elimination of heavy metal promoters (e.g. antimony oxide), and no toxic fume generation

* Corresponding author. Tel./fax: +86 10 6443 4784.
E-mail address: guof@mail.buct.edu.cn (F. Guo).

0032-3861/$ - see front matter © 2007 Elsevier Ltd. All rights reserved.
doi:10.1016/j.polymer.2007.03.044

[12,13]. The flame retardancy mechanism of ATH is based on its thermal decomposition between 200 °C and 400 °C. During this endothermic reaction, ATH releases its chemically bonded water (34.6 wt%), while aluminum oxide remains in the char residue. The water removes the heat energy from the burning zone by changing into vapor, and surrounds the compound surface to lower the concentration of oxygen and burnable gases. Meanwhile, the aluminum oxide provides a protective layer on the surface of the burning material, preventing oxygen and heat reaching it. However, the decomposing temperature of ATH is as low as 220 °C and the efficiency of flame retardancy of ATH is low. So ATH can only be used in those polymers processed at low temperature, and in polyolefin, the overall ATH loading must be higher than 50 wt% to achieve useful flame-retarding properties, which will ruin the mechanical properties of whole material [14,15].

In order to get higher decomposing temperature and better thermal stability, a new kind of aluminum flame retardant as basic aluminum oxalate (BAO) was synthesized by Alcoa (Aluminum Company of America) Company [16]. Recently, another similar aluminum flame retardant as nano-sized hydroxyl aluminum oxalate (nano-HAO) was prepared by using Rotating Packed Bed (RPB) in Research Center of the Ministry of Education for High Gravity Engineering and Technology [17]. The shape of HAO is spindle with the thickness of 85 nm. The decomposing temperature of HAO increases to 320 °C. During the decomposition of HAO, water and non-corrosive gas CO_2 are released. The advantages of nano-HAO are having relatively high decomposing temperature and generating high percent of vapor and gas. But owing to the low percent of Al in nano-HAO there generates low content of aluminum oxide in the char residue, and the rate for forming char is low. In order to make up this demerit, some flame retardants are selected as synergy for nano-HAO, which can improve the process of char formation during decomposition.

Recently, several researches report that polymer/layered silicate (PLS) nanocomposites exhibit remarkable improvement in thermal stabilities when compared with virgin polymer or conventional micro- and macro-composite and thus great interest is focused on them [18–24]. The most commonly used layered silicate is montmorillonite (MMT) and the crystal structure of MMT consists of 1-nm thin layers with a central octahedral sheet of alumina fused between two external silica tetrahedral sheets (the oxygen from the octahedral sheet also belongs to the silica tetrahedral). This layer structure leads to the increase of barrier properties by creating a maze or 'tortuous path' that retards the progress of the gas molecules through the matrix resin [25]. Thus during the thermal decomposition of the composites, MMT can act as a barrier to prevent the oxygen and flammable material getting through. In addition, in the work of Zanetti et al., a catalytic effect of the nano-dispersed clay layers was found to be effective in promoting char-forming reaction in PE/MMT and EVA/MMT [26,27] nanocomposites. So MMT can accelerate the speed of char formation and this char layer can prevent heat and gas from getting through during decomposition effectively. Whereas, if the stacked silicate layers hold heat for so long time, the heat is accumulated and could be used as a heat source to accelerate the decomposition process, in conjunction with the heat flow supplied by the outside heat source [18,28]. This is a demerit of MMT.

From the above, it can be supposed that MMT has some effects on improving the flame retardance properties of nano-HAO. In this paper, we try to introduce MMT into HAO system, firstly, to create barrier between oxygen and material and secondly, to collaborate with HAO to improve the flame retardance. By means of thermal analysis, morphology analysis, FTIR and fire testing, the effect and mechanism of MMT and nano-HAO on flame-retarding LDPE/EPDM system were studied.

2. Experimental section

2.1. Materials

LDPE (Daqing 18D; MFR = 1.5 g/10 min; density = 0.918 g/cm^3) was purchased from Daqing Petrochemical Company (China). EPDM was purchased from DuPont-Dow Elastomers L.L.C. (USA). EVA-*g*-MAH (a type of EVA grafted with 2% maleic anhydride) was manufactured by Ningbo Nengzhiguang New Materials Technology Cooperation (China).

Nano-HAO was produced in the Research Center of the Ministry of Education for High Gravity Engineering and Technology (China), whose molecular formula is shown in Fig. 1. As seen in Fig. 2, nano-HAO is in spindle shape with the thickness of 85 nm. The decomposing temperature of nano-HAO is 320 °C. Montmorillonite (MMT, I.44P) was purchased from Nanocor Inc. (USA).

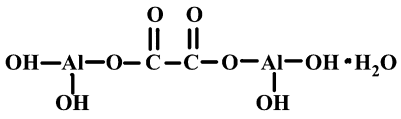

Fig. 1. Molecular formula of nano-HAO.

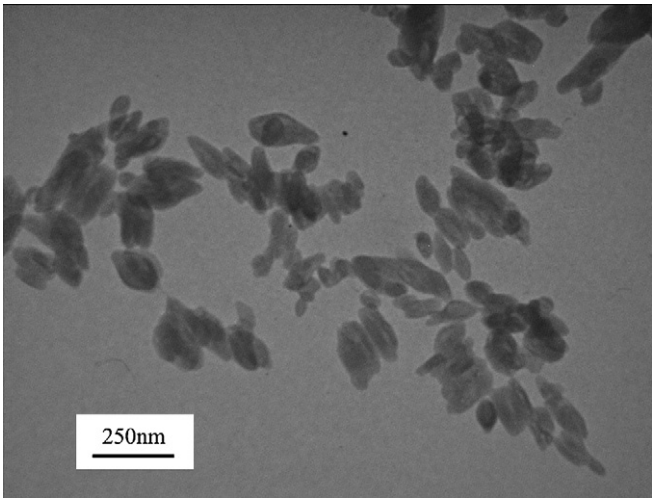

Fig. 2. TEM photo of nano-HAO.

2.2. Preparation of samples

These raw materials were mixed and formed into pellets via a Prism 16 mm twin-screw extruder (TE-20, Coperion Keya (Nanjing) Machinery Co., Ltd, China). The operating temperature of the extruder was kept at 120 °C, 155 °C, 180 °C and 175 °C from hopper to die, respectively, and the screw speed was adjusted to 60 rpm. For test specimen preparation, a single screw extruder (SJ-25, Beijing association of plastic industry, China) was used subsequently. The extruder was operated at the temperature of 120 °C, 155 °C, 180 °C and 175 °C from hopper to die, respectively, with screw speed 50 rpm. Among these composites, one thing should be noted that every 100 g LDPE/EPDM composites contained 14 g EVA-*g*-MAH.

2.3. Characterization of samples

The X-ray diffraction (XRD) analysis was performed using a Rigaku D/max 2500VB2+/PC. An acceleration voltage of 40 kV and 200 mA was applied using Cu Ka radiation. The diffraction angle (2θ) ranges were from 0.5° to 10°.

The morphologies of the composites containing MMT were observed by using the transmission electron microscope (TEM, H-800-1, Hitachi, Japan). The sample was ultramicrotomed with a diamond knife at the room temperature to give 70–90-nm thick section.

The morphologies of nano-HAO and the char layer were observed using the scanning electron microscope (SEM, S-250-III, Cambridge Co., UK) after the specimen was coated with a thin layer of gold.

The thermogravimetric and differential thermal analysis (TG–DTA) data were obtained using a thermogravimetric analyzer (STA-449C, NETZSCH Instruments Co. Ltd, Germany). In each case, a 10–20 mg sample was tested under pure oxygen atmosphere at the heating rates of 5 °C/min, 10 °C/min, 15 °C/min, and 20 °C/min.

The char residue was characterized in triplicate with a Thermo Bruker VECTOR 22 spectrometer using KBr as disperse material. Each sample was scanned for 32 times with a resolution of 4 cm^{-1}. All the spectra were scanned within the range 400–4000 cm^{-1}.

The flame retardancy of all samples was evaluated by the tests of limiting oxygen index (LOI) and UL94 test. The LOI values were calculated by using oxygen index instrument (HC-22, Jiangning Analysis Instrument Factory, China) according to ISO 4589-1984 standard, and sample dimensions were measured as $100 \times 10 \times 4$ mm. UL94 tests were performed on integrated horizontal testing apparatus (CZF-3, Jiangning Analysis Instrument Factory, China), with sample dimensions as $125 \times 10 \times 4$ mm according to ANSI/UL 94–2001 standard.

2.4. Calculation of activation energy

In the non-isothermal experiments carried out with a thermo balance, the sample mass is measured as a function of temperature. The rate of degradation or conversion, $d\alpha/dt$, is a linear function of a temperature-dependent rate constant, k, and a temperature-independent function of conversion, α, that is,

$$\frac{d\alpha}{dt} = kf(\alpha) \tag{1}$$

The reaction rate constant k has been described by the Arrhenius expression:

$$k = A\exp\left(-\frac{E}{RT}\right) \tag{2}$$

where A is the pre-exponential factor, E is the activation energy, R is the gas constant, and T is the absolute temperature.

The combination of Eqs. (1) and (2) gives

$$\frac{d\alpha}{dt} = Af(\alpha)\exp\left(-\frac{E}{RT}\right) \tag{3}$$

If the temperature of the sample is changed by a controlled and constant heating rate, $\beta = dT/dt$, the variation in the degree of conversion can be analyzed as a function of temperature, this temperature being dependent on the time of heating.

Therefore, the rearrangement of Eq. (3) gives

$$\frac{d\alpha}{dT} = \frac{A}{\beta}f(\alpha)\exp\left(-\frac{E}{RT}\right) \tag{4}$$

The integrated form of Eq. (4) is generally expressed as

$$g(\alpha) = \int_0^{\alpha}\frac{d\alpha}{f(\alpha)} = \frac{A}{\beta}\int_0^{T}\exp\left(-\frac{E}{RT}\right)dT \tag{5}$$

where $g(\alpha)$ is the integrated form of the conversion dependence function.

The integral method involves an approximate integration of Eq. (5). Flynn–Wall–Ozawa method is applied. The Flynn–Wall–Ozawa method using the Doyle's approximation for the integration has been expressed as:

$$\log\beta = \log\left[\frac{AE}{g(\alpha)R}\right] - 2.315 - 0.4567\frac{E}{RT} \tag{6}$$

Using Eq. (6), the linear representation of $\log\beta$ versus $1/T$ allows us to determine the activation energy with a given value of the conversion.

The advantage of Flynn–Wall–Ozawa method is that the reaction order is out of consideration during the calculation. So, the process of calculation is simplified and the results are veracious.

3. Results and discussion

3.1. Fire testing results

3.1.1. Effects of nano-HAO and MMT on the flame retardancy of LDPE/EPDM composites

The effects of nano-HAO and MMT on LOI of LDPE/EPDM composites are compared in Fig. 3. When the content

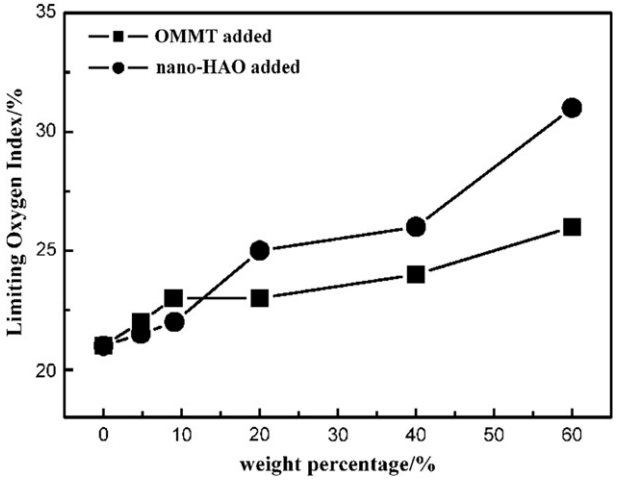

Fig. 3. Effects of nano-HAO and MMT on LOI of the composites.

of flame retardants increased from 0% to 60%, the LOI of the composites containing nano-HAO increased from 22.0 to 31.0, and the LOI of the composites containing MMT just increased from 22.0 to 26.0. Obviously, nano-HAO was more effective than MMT in enhancing LOI value of the composites.

During the UL94 test, the flammability of all the specimens was classed as UL94HB and the results are summarized in Table 1. Apparently, with the increase of the content of flame retardants, the calculated linear burning rates of the specimens decreased. During the combustion, the spreading rate of flame was associated with the amount of heat and flammable gas accumulated. Nano-HAO acted as heat remover and flammable gas diluter with the release of water and carbon dioxide after decomposing, while MMT mainly acted as heat and gas barrier. At the low loading level, the performance of nano-HAO acting as heat remover and gas diluter was more effective than that of MMT acting as barrier in inhibiting the flame, so as seen in Table 1, the linear burning rates of the nano-HAO/LDPE/EPDM composites was obviously less than that of MMT/LDPE/EPDM composites. When the content of flame retardant reached 40%, the burning rates of nano-HAO/LDPE/EPDM composites and the MMT/LDPE/EPDM composites were at the same level, indicating that the performance of MMT as barrier could be as effective as that of nano-HAO as heat remover and gas diluter in inhibiting the flame. When the content of flame retardants increased to 60%, such high loading level leads to the fact that nano-HAO not only could act as heat remover and gas diluter, but also could act as heat and gas barrier, while MMT only could act as heat and gas barrier. So the composites with nano-HAO could be self-extinguished, while the composites with MMT were still burning without ceasing. Along with the burning, the composites containing MMT were easy to form char together with heavy smoke and the composites containing nano-HAO didn't smoke but the char residue cannot keep in shape. As a whole, nano-HAO exhibited better performance than what MMT did in inhibiting flame.

Table 1
Results of UL94 horizontal burning test (UL94HB)

Content/%	The calculated linear burning rate/mm min^{-1}	
	MMT	nano-HAO
0	33.25 ± 2.35	33.25 ± 2.35
4.8	30.89 ± 3.17	27.00 ± 1.00
9.1	32.25 ± 3.70	25.74 ± 3.83
20	28.15 ± 3.87	23.97 ± 1.67
40	22.60 ± 0.32	22.78 ± 0.82
60	16.76 ± 1.48	10.73 ± 0.32[a]

[a] During this test, this sample's flame front ceased before 25 mm mark and the damaged length was 17.0 ± 0.5 mm. The other samples' flame passed the 100 mm mark.

3.1.2. Synergistic effects of MMT and nano-HAO on the flame retardancy of LDPE/EPDM composites

The influence of MMT on the flame retardancy of nano-HAO/LDPE/EPDM composites is shown in Table 2, and the content of nano-HAO was kept at 50%. When the weight percentage of MMT ranged from 0% to 10%, the LOI value of the composites increased slightly and the flammability of the composites was classed as UL94HB with the damaged length decreasing. In addition, during the process of combustion, there formed compact char on the surface. With the increase of MMT content, the time for char formation became short.

In Fig. 4, the flame retardancy of the composites filled with the same weight percentage of nano-HAO or nano-HAO/MMT flame retardants is compared. As seen in Fig. 4(a), with the increase of the proportion of MMT and nano-HAO, the LOI value increased firstly and dropped later. When the proportion of MMT and nano-HAO was 1:3, the LOI of the composites was 34.0, while the LOI of the composites with 60% nano-HAO was 31.0 and the LOI of the composite with 60% MMT was 26.0. In Fig. 4(b), as to the burning behaviors, though the flame retardancy of the composites still kept at the UL94HB level, the elapse time for horizontal burning decreased greatly when MMT was added together with nano-HAO in the composites. In the histogram, when 10% MMT substituted 10% nano-HAO in the nano-HAO/LDPE/EPDM composites, the elapse time for combustion decreased sharply

Table 2
Flame retardancy of nano-HAO/MMT/LDPE/EPDM composites[a]

Content of MMT/%	LOI/%	UL94 test results
0	30	UL94HB: flame passed the 100 mm mark and the calculated linear burning rate was 17.57 ± 0.30 mm min^{-1}
3	30	UL94HB: flame passed the 25 mm mark but ceased before 100 mm mark. The damaged length was 26.0 ± 0.5 mm
5	31	UL94HB: flame ceased before 25 mm mark and the damaged length was 23.0 ± 0.3 mm
8	31.5	UL94HB: flame ceased before 25 mm mark and the damaged length was 15.1 ± 1.0 mm
10	32	UL94HB: flame ceased before 25 mm mark and the damaged length was 16.0 ± 1.0 mm

[a] The content of nano-HAO was kept at 50 wt%. LDPE and EPDM were in the proportion of 7:3.

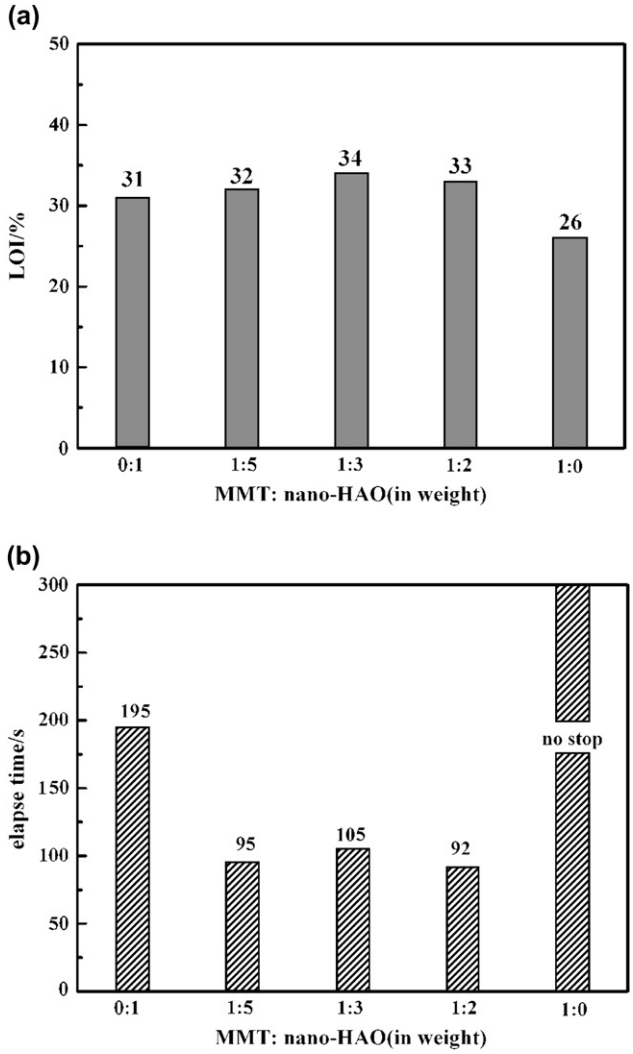

Fig. 4. The flame retardancy of the composites filled with 60 wt% fillers (a) LOI results; (b) UL94 horizontal burning tests' results.

from 195 s to 95 s, while the flame on the composites containing 60% MMT could not cease. Such results reflected the synergistic effect of nano-HAO and MMT on flame retarding the composites.

3.2. Dispersing state of MMT in the composites

When 20% MMT was added into the composites together with 40% nano-HAO, the XRD pattern of these composites was scanned, which was used to compare with the XRD pattern of the pure MMT, as seen in Fig. 5. It could be found that the basal spaces of nanocomposites increased to 3.99 nm from 2.83 nm of the original MMT, which was attributed to the fact that the macromolecular chains have intercalated into the MMT galleries. Furthermore, the TEM photo of the composites, as shown in Fig. 6, presented the intercalation structure of MMT in the MMT/nano-HAO/LDPE/EPDM composites, which was consistent with the results of XRD.

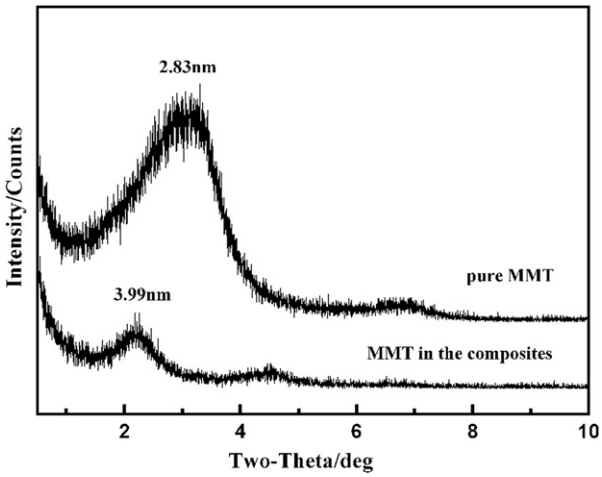

Fig. 5. XRD patterns of MMT and the MMT/nano-HAO/LDPE/EPDM composites.

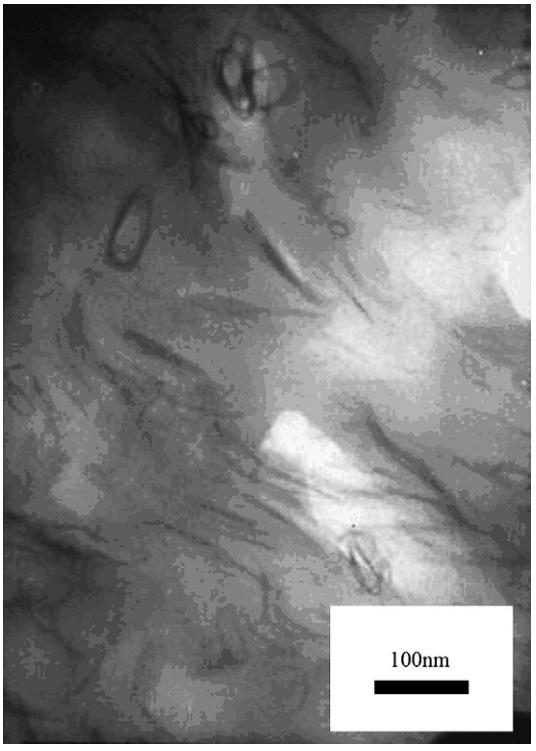

Fig. 6. TEM photo of the composites containing 10% MMT.

3.3. Thermal analysis

The thermooxidative degradation of MMT/nano-HAO/LDPE/EPDM composites was carried out in oxygen atmosphere at the heating rate of 10 °C/min. The TG and DTA curves are shown in Fig. 7. As shown in the curves, when nano-HAO was added into LDPE/EPDM composites, there was 30% residue left and the heat energy released decreased. When MMT was added further, there was more residue generated and the heat energy released decreased greatly. Meanwhile, the decomposing temperature of the composites at 5%

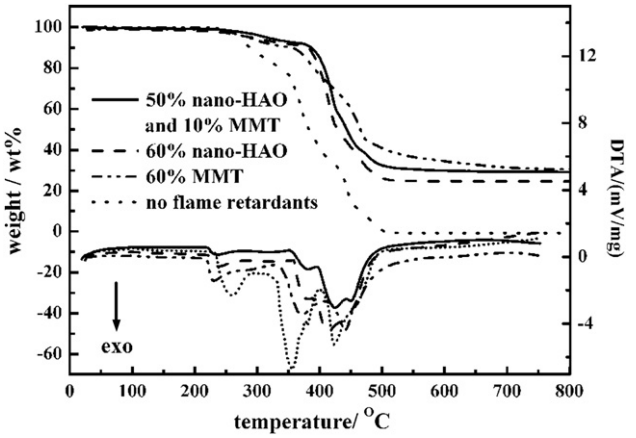

Fig. 7. TG and DTA curves of the composites filled with different contents of flame retardants.

weight loss enhanced from 288.7 °C to 316.1 °C after MMT was added.

Additionally, from the TG data at different heating rates β ($\beta = 5$ °C/min, 10 °C/min, 15 °C/min or 20 °C/min), the activation energies of decomposition were calculated by Flynn–Wall–Ozawa method (as seen in Section 2.4). At given value of the conversion, the activation energy can be obtained from a logarithmic plot of heating rates as a function of the reciprocal of temperature, since the slope of such a line is given by $-0.4567\ E/R$. For the present work, the conversion values of 5%, 10%, 20%, 30%, 40%, 50%, 60%, 70%, 80% and 90% were used. Fig. 8 shows the fitting lines of the MMT/nano-HAO/LDPE/EPDM composites at the selected conversion values. All of the calculated activation energies are listed in Fig. 9 and during the linear fitting, results showed that the correlation coefficient was more than 0.990.

As shown in Fig. 9, at the 5% conversion, because MMT had good thermal stability, its addition resulted in the increase of the calculated activation energy of the composites by 20.8 kJ/mol. Nevertheless, before the 70% conversion, the addition of MMT resulted in no changes in the activation

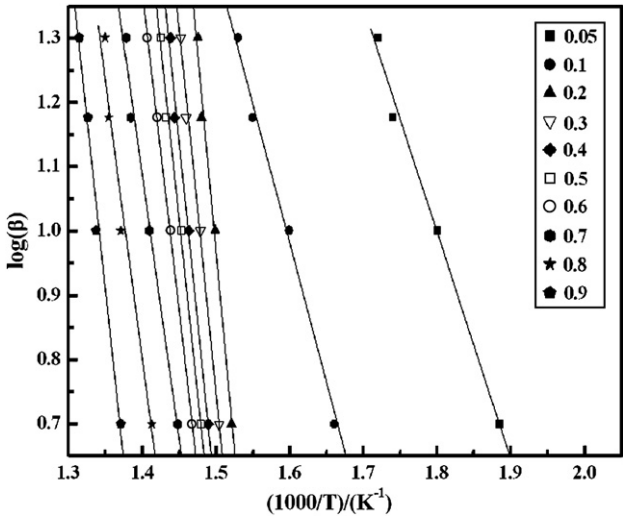

Fig. 8. Flynn–Wall–Ozawa plots at varying conversion.

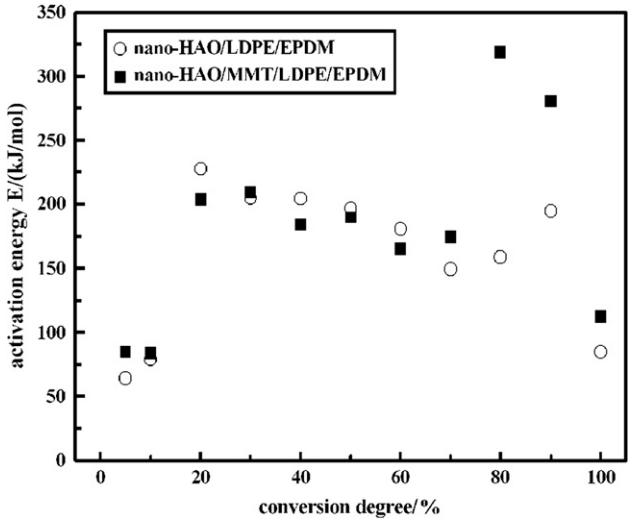

Fig. 9. Calculated activation energies at various weight loss of the decomposition.

energies of the composites. Until the conversion was more than 80%, the activation energy of the composites containing MMT was almost as twice as that of the composites without MMT. Such great enhancement of activation energy was attributed to the fact that there formed ceramic-like char residue from MMT/polymer, which had good thermal stability and good barrier property, and then the macromolecules could be protected.

Therefore, adding MMT into the composites could enhance the activation energy apparently, and thus the thermal stability of the composites was improved.

3.4. FTIR analysis

In Fig. 10, the FTIR spectral results of residues of the composites under the char layer after thermally treated at 300–450 °C for 4 min separately are shown, which were used to illustrate the protection of the formation of char layer in retarding the degradation of the composites. MMT/nano-HAO/LDPE/EPDM composites (a) and nano-HAO/LDPE/EPDM composites (b) were used for this experiment. The peak positions and assignments of FTIR spectra are listed in Table 3.

As shown in Fig. 10(a), the intensity of the peaks corresponding to the stretching vibration, bending vibration and rocking vibration of C–H bond belonging to the CH_2 group of polymer matrix, which is at 2910 cm^{-1}, 2850 cm^{-1}, 1465 cm^{-1}, 1365 cm^{-1} and 720 cm^{-1}, respectively, decreased obviously and at 1591 cm^{-1}, a new peak assigned to C=C bond stretching vibration appeared when the temperature reached 400 °C, which inferred that the crosslinking carbonisation occurred during the decomposition of the polymer matrix [29]. Simultaneously, the intensity of the peaks at 3659 cm^{-1}, 3597 cm^{-1} and 3473 cm^{-1}, which was assigned to the stretching vibration of O–H bond in nano-HAO molecule (Fig. 1) decreased with the increase of treating temperature. When the temperature was up to 400 °C, there appeared a broad peak at 3333 cm^{-1} corresponding to the O–H bond in free water.

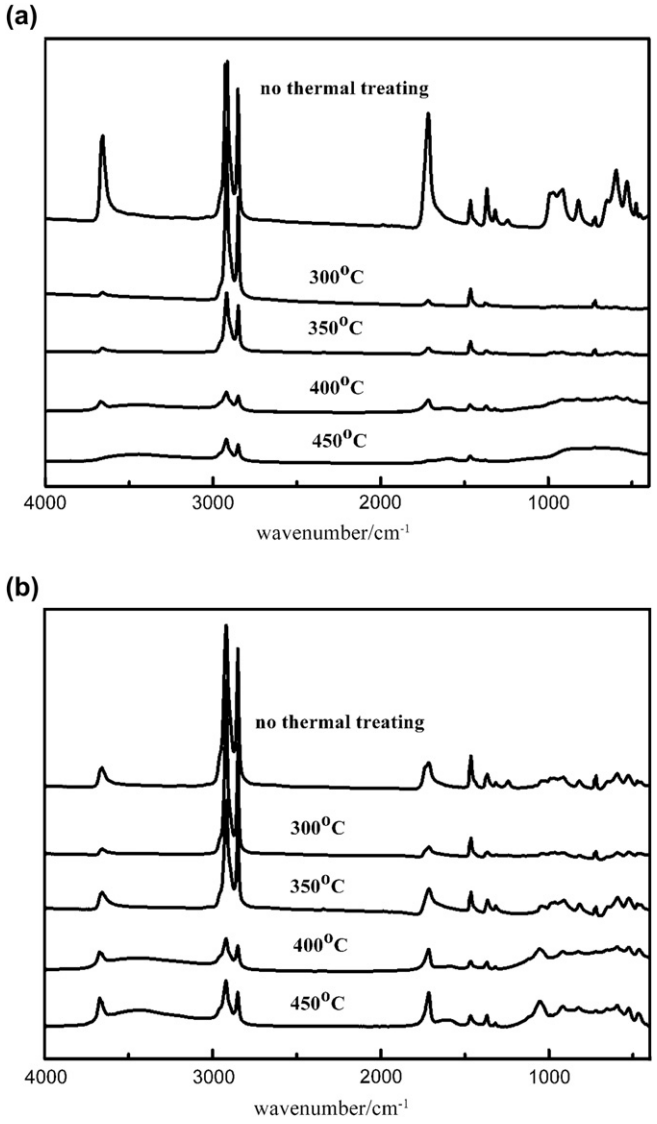

Fig. 10. FTIR spectra of LDPE/EPDM composites residue (a) nano-HAO/LDPE/EPDM composites; (b) nano-HAO/MMT/LDPE/EPDM composites.

Meanwhile, the intensity of the peak at 1716 cm^{-1}, which was assigned to stretching vibration of C═O bond in nano-HAO, decreased and almost disappeared at 450 °C. These spectral results suggested that when the composites were treated at 450 °C for 4 min, nano-HAO decomposed totally with the release of water and carbon dioxide.

When the composites contained MMT, the FTIR spectra showed that the intensity of the peak corresponding to the Si–O bond at 1055 cm^{-1} increased, which indicated that the inorganic-rich carbonaceous silicate char formed in the composite [30]. At the same time, the intensity of the peaks corresponding to the O–H bond decreased, but these peaks still existed with the appearance of the peak at 3333 cm^{-1} at 450 °C. Similarly, the intensity of the peak corresponding to C═O bond decreased, but these peaks didn't disappear when the temperature was 450 °C. With the comparison between the changes of the peaks corresponding to C═O bond and O–H bond in Fig. 10(a) and (b), we found that the decrease of the intensity of these peaks in MMT/nano-HAO/LDPE/EPDM composites was less than that of the peaks in nano-HAO/LDPE/EPDM composites, which indicated that the degree for the decomposition of nano-HAO decreased where MMT helped the composites to generate carbonaceous silicate char. At the same time, with the appearance of the new peak at 1591 cm^{-1} corresponding to C═C bond at 400 °C, the decrease of the peaks at 2910 cm^{-1}, 2850 cm^{-1}, 1465 cm^{-1}, 1365 cm^{-1} and 720 cm^{-1} corresponding to C–H bond was less than what was shown in FTIR spectra of nano-HAO/LDPE/EPDM composites, which referred that the crosslinking carbonisation in the polymer matrix was improved. Combining these results above together, we can deduce that when MMT was added into the composites, the barrier effect of the char layer was improved and thus the decomposition of nano-HAO and polymer matrix under the char layer was retarded.

Table 3
Major absorbance peaks and assignments in FTIR spectroscopy

Peak position (cm^{-1})		Appearance in materials	Assignments
Nano-HAO/LDPE/EPDM	Nano-HAO/MMT/LDPE/EPDM		
3659	3659	Nano-HAO, MMT	ν(O–H) (free), ν(O–H)
3597	3597	Nano-HAO, MMT	Intramolecular H-bond, ν(O–H)
3473	3473	Nano-HAO, MMT	Intermolecular H-bond
3333	3333	Nano-HAO, MMT	ν(O–H) (water)
2910	2919	LDPE, EPDM	$\nu_{as}(CH_2)_a$
2850	2850	LDPE, EPDM	$\nu_s(CH_2)_s$
1716	1715	Nano-HAO	N(C═O)
1591	1584		N(C═C)
1465	1463	LDPE, EPDM	$\delta(CH_2)_{as}$
1365	1366	LDPE, EPDM	$\delta(CH_2)_s$
1317	1317	Nano-HAO	$\nu(COO^-)_s$
1241	1242	LDPE, EPDM	ν(C–C)
	1055	MMT	ν(Si–O–Si)
970	969	Nano-HAO	δ(OH)
914	911–916	Nano-HAO, MMT	δ(OH)
820	819	Nano-HAO, MMT	ν(Al–O)
720	720	LDPE, EPDM	$r(CH_2)_a$
475,527,594	474,526,593	Nano-HAO, MMT	ν(Al–O)
	465	MMT	δ(Si–O)

3.5. Morphology characterization of the char layer

The SEM photos of char layer, as shown in Fig. 11, were taken after the specimens finished their combustion in air. When only nano-HAO was added, the char structure was porous and easy to be deformed (Fig. 11(a)). This porous char structure was beneficial to the release of CO_2 and H_2O, which was generated after nano-HAO decomposed, while the heat and oxygen transfers were promoted at the same time. When MMT was added individually, the compact, ceramic-like and carbonaceous silicate char (Fig. 11(b)) was formed on the surface of the composites. This structure could prevent the heat and gas from getting through. When nano-HAO and MMT were added together, there formed a laminated structure in the char (Fig. 11(c)). The holes in the

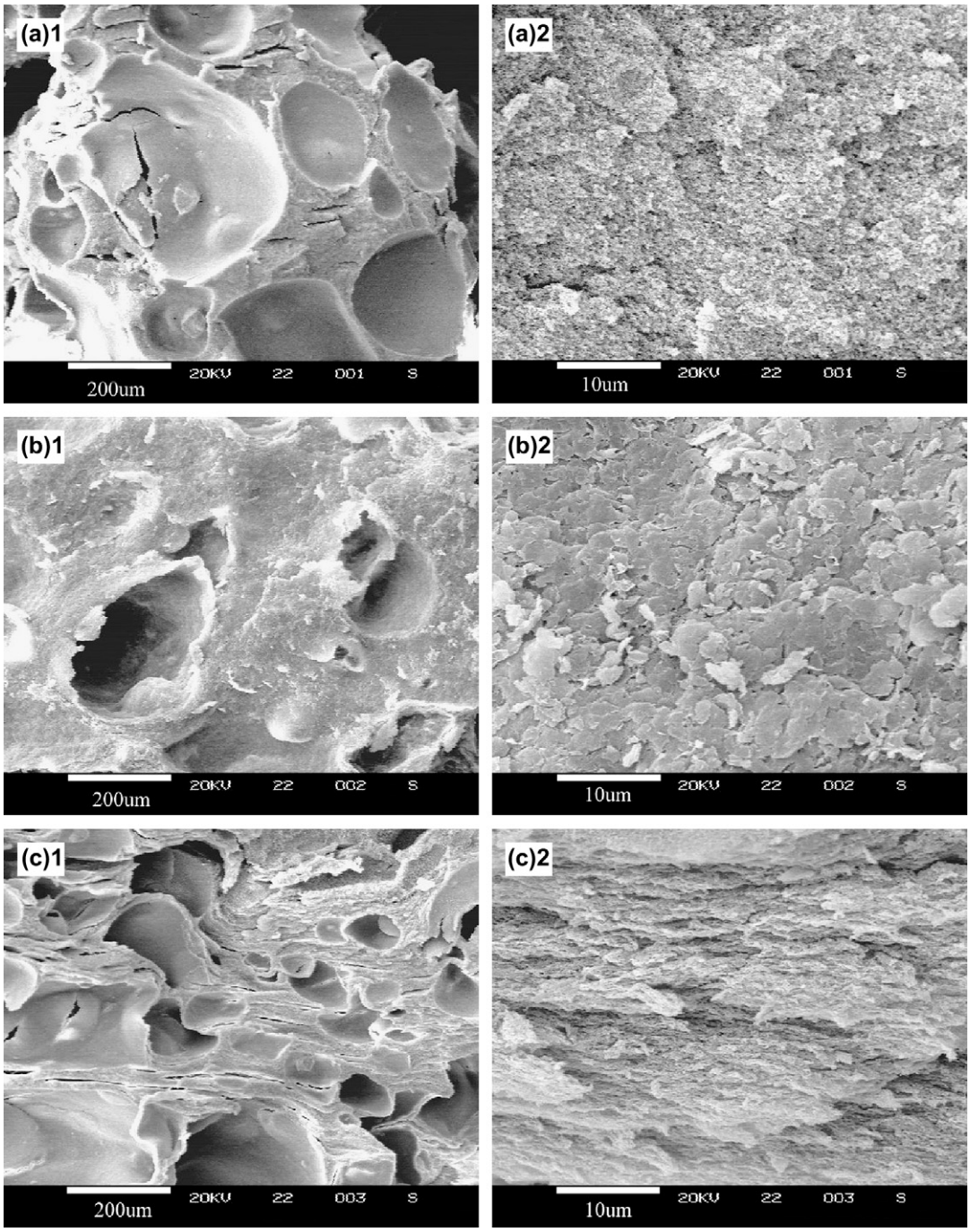

Fig. 11. SEM photos of the char layer after the composites combusted (a) composites containing 60% nano-HAO; (b) composites containing 60% MMT; (c) composites containing 50% nano-HAO and 10% MMT.

char became small and the char was stiffened. This laminated structure not only reduced the transition speed of heat and oxygen, but also slow down the releasing speed of CO_2 and H_2O, which could dilute the flammable gas in the gas phase longer.

3.6. Mechanism proposal

From the thermal analysis and the UL94 tests, the flame retardancy of the composites was found to be improved because the thermal stability was enhanced by adding MMT. Then by means of FTIR and SEM analysis, mechanism was proposed for this improvement. It was illustrated as the fact that the structure of char layer was adjusted with the addition of MMT, and thus the transfer of gas and heat was retarded, which is further presented in Fig. 12.

In such sketch map, MMT makes the char to be compact, which could stop the combustion by preventing oxygen reaching the surface of the burning composites. At the same time, the heat was kept around the composites also, and thus heat

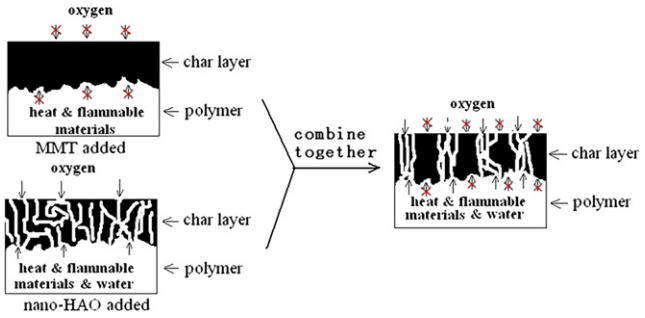

Fig. 12. Mechanism of synergistic effect on flame retardancy.

was accumulated to support the combustion again. So as shown in Section 3.1.1, MMT could not be used as flame retardant alone.

As to nano-HAO, it helped the composites to form many holes in the char layer, which helped the vapor and heat to pass through quickly. But this structure had two demerits: one was that these large holes became the stress concentration point in the char, which resulted in the brittleness of the char and the other was that the oxygen could pass through the char layer easily.

When MMT and nano-HAO were mixed and used as flame retardants together, there formed a laminated structure in the char layer. The density of the char varied with the distribution of nano-HAO and MMT in the composites. The part with high content of nano-HAO had many small holes, and the part with high content of MMT was compact. As we know, if the content of heat and mass was under a limitation, the fire would be extinguished. Therefore, heat and mass need not be transmitted completely. According to this idea, this structure was useful. The laminated structure could adjust transmission speed to an optical level. On this level, content of oxygen, flammable materials, and heat were not enough to support the combustion. What's more, by changing the content of MMT and the distribution of MMT, the rate of heat and mass transmittance could be controlled and adjusted.

4. Conclusions

The synergistic effect of MMT and nano-HAO on flame retarding the LDPE/EPDM composites was investigated in this paper. By means of LOI tests and UL94 horizontal burning tests, it was found that the addition of MMT can produce synergistic effect on flame-retarding nano-HAO/LDPE/EPDM system. When the weight percentage of MMT reached 10% and the content of nano-HAO was kept at 50%, the LOI of the composites was up to 32.0, and the flame was self-extinguished with the damaged length of 16 ± 1.0 mm. Through the analysis of TG–DTA, FTIR and SEM, it was proved that the barrier effect of the char layer was promoted when MMT was added and thus the decomposition of nano-HAO and polymer matrix under the char layer was retarded.

Acknowledgement

This work is financially supported by the 863 Project Foundation of China, Grant No. 2002AA302605.

References

[1] Grand AF, Wilkie CA. Fire retardancy of polymeric materials. 1st ed. New York: Marcel Dekker; 2000 [chapter 2].
[2] Chigwada G, Jash P, Jiang DD, Wilkie CA. Polym Degrad Stab 2005;88:382–93.
[3] Finberg I, Yaakov YB, Georlette P. Polym Degrad Stab 1999;64:465–70.
[4] Rosa ADL, Recca A, Carter JT, McGrail PT. Polymer 1999;40:4093–8.
[5] Smith R, Georlette P, Finberg I, Reznick G. Polym Degrad Stab 1996;54:167–73.
[6] Liaw DJ, Chang P. Polymer 1997;38:5545–50.
[7] Georlette P. Plast Addit Compound 2001;3:28–33.
[8] Hippi U, Mattila J, Korhonen M, Seppälä J. Polymer 2003;44:1193–201.
[9] Pinto UA, Visconte LLY, Nunes RCR. Eur Polym J 2001;37:1935–7.
[10] Du L, Qu B, Xu Z. Polym Degrad Stab 2006;91:995–1001.
[11] Lu H, Hu Y, Yang L, Wang Z, Chen Z, Fan W. Macromol Mater Eng 2004;289:984–9.
[12] Zilberman J, Hull TR, Price D, Milnes GJ, Keen F. Fire Mater 2000;24:159–64.
[13] Lynch TJ, Chen T, Riley D. Reinf Plast 2003;47:44–6.
[14] Camino G, Maffezzoli A, Braglia M, Lazzaro MD, Zammarano M. Polym Degrad Stab 2001;74:457–64.
[15] McGarry K, Zilberman J, Hull TR, Woolley WD. Polym Int 2000;49:1193–8.
[16] Stinson JM. J Vinyl Addit Technol 1995;1:94–8.
[17] Ma S, Guo F, Chen J. J Chem Eng Chin Univ 2005;19:244–7.
[18] Qiu L, Chen W, Qu B. Polymer 2006;47:922–30.
[19] Zhang Z, Zhang L, Li Y, Xu H. Polymer 2005;46:129–36.
[20] Wan C, Tian G, Cui N, Zhang Y, Zhang Y. J Appl Polym Sci 2004; 92:1521–6.
[21] Ding P, Qu B. Polym Eng Sci 2006;46:1153–9.
[22] Stretz HA, Paul DR, Cassidy PE. Polymer 2005;46:3818–30.
[23] Stretz HA, Paul DR, Li R, Keskkula H, Cassidy PE. Polymer 2005; 46:2621–37.
[24] Yalcin B, Cakmak M. Polymer 2004;45:6623–38.
[25] Shah RK, Krishnaswamy RK, Takahashi S, Paul DR. Polymer 2006; 47:6187–201.
[26] Zanetti M, Bracco P, Costa L. Polym Degrad Stab 2004;85:657–65.
[27] Zanetti M, Costa L. Polymer 2004;45:4367–73.
[28] Ray SS, Bousmina M. Prog Mater Sci 2005;50:962–1079.
[29] Xie R, Qu B. J Appl Polym Sci 2001;80:1190–7.
[30] Qin H, Zhang S, Zhao C, Feng M, Yang M, Shu Z, et al. Polym Degrad Stab 2004;85:807–13.